The charging behaviour and internal electric field of PMMA irradiated by a kiloelectronvolt electron beam

1995 J. Phys.: Condens. Matter 7 1129

(http://iopscience.iop.org/0953-8984/7/6/014)

J. Phys.: Condens Matter 7 (1995) 1129–1137. Printed in the UK

The charging behaviour and internal electric field of PMMA irradiated by a kiloelectronvolt electron beam

H Chen, H Gong and C K Ong

Department of Physics, National University of Singapore, 10 Kent Ridge Crescent, Singapore 0511, Singapore

Received 13 July 1994, in final form 21 September 1994

Abstract. A scanning electron microscope (SEM) is employed in the investigation of the charging behaviour of polymethylmethacrylate (PMMA) specimens. Charges trapped in the PMMA specimens are measured using the SEM mirror image method under different conditions of radiation time, accelerating voltages and beam currents. The influence of the surface potential established and the internal electric field arising in the PMMA specimen is studied, and the latter is found to play a more important role. There exists a saturation value for the charge that can be trapped in the specimen under a fixed charging condition. Beyond the saturation value, the trapped charge destabilizes and surface discharge is observed. A Gaussian model of charge distribution is used for the calculation of the electric field. The strength of the electric field initiating surface discharge is estimated.

1. Introduction

The study of the charging process is closely related to and hence of great help in the understanding of breakdown and surface flashover phenomena [1–3]. In the charging process when a specimen is subjected to an electron beam and charged, the charge trapped in the specimen creates a surface potential as well as an internal field radiating from the charge centre. During a continuous charging process, the surface potential arising from the space charge decelerates the injecting electrons and reduces the electron penetration range. As a result, the space charge distribution is formed. It may also be possible, at least theoretically, for the surface potential to be high enough to repel all the incoming electrons [4]. On the other hand, the internal field built up in the charged specimen increases as the space charge increases. The arising field may reach a critical value E_c, at which it is able to detrap electrons trapped in the specimen [5]. If the internal field increases further to reach the value E_m [5], the trapping and detrapping process will reach an equilibrium and the total space charge will not increase any further. The magnitude of the internal field depends on the space charge distribution [6] and the location in the specimen. Both the surface potential and the internal field are interrelated and play important roles in the charging as well as the discharging process. However, the question remains: which parameter, the surface potential or the internal field, plays the more important role in describing the charging and even the discharging processes?

In the study of the flashover (surface breakdown) mechanism, the electron cascade model is most popular, in which breakdown is believed to be initiated by electrons accelerated in an electric field, forming an electron cascade [7–9]. However, this mechanism requires the generation of electrons heated by an accelerating field (hot electrons) whose energy must be sufficient to produce electron–hole pairs by impact [10]. Investigations on the problem of hot

0953-8984/95/061129+09$19.50

electrons in wide-band-gap insulators have led to the conclusion that the impact ionization requires the application of electric fields greater than 1 MV cm^{-1} [11, 12]. Because this value is far beyond the flashover voltage in most practical situations, the electron cascade model has been a matter of controversy for 30 years [13] even though the effect of the hot electrons in the dielectric breakdown is affirmed by some experimental work [14].

Polymethylmethacrylate (PMMA) is an important insulating material and has been investigated by several workers [15–17]. Zahn *et al* used the Kerr electro-optic field mapping technique to measure the charge distribution and electric field distribution along the depth of PMMA samples irradiated by broad megaelectronvolt electron beams [16, 17]. In contrast, we investigate the charging process of PMMA irradiated by a fine beam of kiloelectronvolt electrons and the associated internal electric field in the radial direction of the trapped charge. The investigation is performed by employing the mirror image method (MIM) [18, 19] through the use of a scanning electron microscope (SEM). Firstly, we demonstrate that there exists a saturation value for the charge that can be trapped in the specimen under a fixed charging condition. Secondly, we illustrate that the internal field established by the trapped charge limits the value of saturation charge. Lastly, we proceed to estimate the value of electric field that initiates the surface discharge.

It is appropriate to clarify some of the terms used in this research field. In general, dielectric breakdown indicates the electrical breakdown through the specimen and surface breakdown (flashover) means the voltage breakdown along the surface of insulators [3]. In our work we are concerned with surface discharge, the transport of charge from the accumulated space charge region in the specimen as is studied by Le Gressus *et al* [1, 20]. Charge is implanted by a fine electron beam of kiloelectronvolt energy and trapped in a small area of the order of micrometres near the surface, so discharge takes place along the surface of the specimen. As the discharge from an accumulated space charge can even cause the bulk breakdown of a dielectric [20, 21], our study on surface discharge is closely related to the field of dielectric breakdown and electrical insulation. The advantages of using the SEM include the ease in selecting charging conditions, such as the energy, the current of incident electron probe, and the small yet controllable area of charge concentration. The use of SEM techniques for the investigation of charging is widely accepted and several valuable results have been obtained [1, 5, 18, 22].

2. Experiment

The electron beam of an SEM in the static mode is employed to charge the PMMA specimens. Charges trapped in the specimens are measured by the MIM method. The mirror effect in an SEM due to trapped charge was first reported by Vigoroux *et al* in 1985 [23]. When an insulator specimen is charged by an electron beam in an SEM, a potential distribution due to the trapped charge is set up. If the specimen is scanned by an electron beam accelerated at low voltage, the incident electrons can be reflected by the repelling potential of the trapped charge. For a given incident direction, the beam is reflected and hits one spot of the SEM chamber. This hit generates secondary electrons that are collected by the secondary-electron (SE) detector of the microscope. As different incident beam directions are related to different spots of the microscope chamber, an image of the chamber is obtained when the SEM is operated in the secondary-image mode. The obtained image is related to the electron trajectory and thus related to the trapped charge in the specimen. This makes it possible to measure the charge by producing a mirror image in the SEM. The details of the MIM method can be found in our previous work [18, 19]. Here we focus on some aspects of the experimental details.

Prior to the experiment, the surface of the PMMA specimens is scrupulously cleaned using hexane and distilled water. After being gently baked under a 500 W incandescent light, the specimens are then transferred into a vacuum chamber, where they are kept for a few days to ensure that all the moisture has been driven out. The specimen, of dimensions 10×10 mm^2 in width and 5 mm thick, is mounted on the earthed specimen holder and the free upper surface is perpendicular to the electron beam. A Jeol 50A-LNB liquid nitrogen baffle is employed to keep a clean vacuum. Experiments are performed at room temperature. The specimen is only charged once and is not used again.

To ensure the repeatability and reliability of the charging condition and experimental results, a series of standard steps is followed in the experiments. These include the following: (i) An optical microscope attached to the SEM is used to examine the specimen surface. This makes it possible to choose an ideal area on the specimen surface for the charging experiment. (ii) The optical microscope is also used to help to focus the electron beam without the beam directly hitting the specimen surface. The electron beam is focused to less than 0.5 μm in diameter. (iii) The beam current is measured and calibrated by the use of a Faraday cup. (iv) To monitor the emitted secondary and backscattered electrons during the charging process, the SE detector of the SEM is switched on to record the signal received. This information is of great value in understanding the charging process and will be elaborated further in section 5.

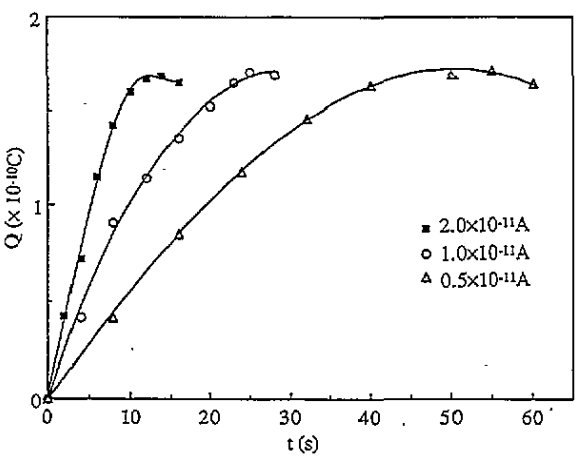

Figure 1. The time dependence of charges trapped in PMMA specimens with fixed charging voltage $U_0 = 39$ kV and different charging currents $I = 0.50 \times 10^{-11}$, 1.0×10^{-11}, and 2.0×10^{-11} A. The experimental data are presented as symbols.

3. The effect of beam current on the charging behaviour

The PMMA specimens are charge with fixed accelerating volgate $U_0 = 39$ kV with three different charging currents, $I = 0.50 \times 10^{-11}$, 1.0×10^{-11}, and 2.0×10^{-11} A. Charge Q trapped in the specimens with increasing radiation time t is measured. The results are shown in figure 1. Charge Q increases with t. The increasing slopes of the three curves are different due to the different charging currents but they reach the same saturation value $Q_s = 1.7 \times 10^{-10}$ C. Beyond the saturation value, charge destabilization and surface

discharge are observed and the MIM measurement is no longer consistent and does not give repeatable results.

We classify the experimental results into three stages (see figure 1). In stage I, charge Q trapped in the specimen increases linearly as the radiation time t increases and follows the line $Q_t = It$ (total injected charges) closely. Since the secondary and backscattered electron yields are much smaller than unity for such high-energy electron beam incidence, most of the injected electrons remain implanted in the specimen. In stage II, Q increases as t increases but deviates from the straight line $Q_t = It$. In polymers, electrons are trapped in energetically discrete trapping levels with a random distribution of trap depths [24, 25]. With the accumulation of charges in the specimen, the internal electric field is built up and eventually increases to E_c at the edge of the charge distribution. By then, electrons trapped in the shallow traps in that particular spot or near defect sites can be released. This caused the deviation of the charge Q from the total injected charge Q_t. However, the detrapping process is a localized event. The internal field established is still not large enough to cause a large quantity of electrons to be released and the charges trapped in the specimen are still stable. In stage III, Q does not increase with t and approaches the same saturation value for three different incident beam currents. This means that there exists a charge limit (Q_s) for a given material at a given incident beam energy (U_0). The value of Q_s depends on U_0 but not beam current. As Q_s is reached, the corresponding field E_m is large enough to destabilize the space charge distribution. As a trapped electron is released by E_m from the edge of the distribution or near defect sites, the stored polarization and distortion energies are released [1]. This causes local heating in the specimen and hence the trapped electron will be more mobile as the temperature rises. Consequently, an avalanche of detrapped electrons is initiated. This leads to space charge collapse and surface discharge.

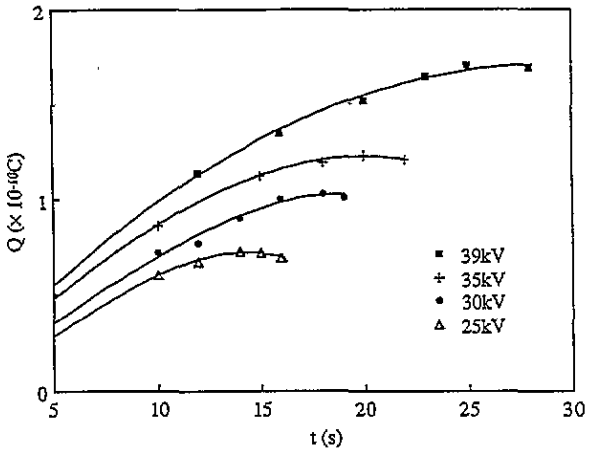

Figure 2. The time dependence of charges trapped in PMMA specimens with fixed charging current $I = 1.0 \times 10^{-11}$ A, and different charging voltages $U_0 = 25$, 30, 35, and 39 kV. The experimental data are presented as symbols.

4. The effect of beam energy on the charging behaviour

By changing the accelerating voltage of the electron beam, we investigate the effects of the beam energy on the charging process. Figure 2 shows the results for charge Q versus

radiation time t with fixed charging current $I = 1.0 \times 10^{-11}$ A and with four different accelerating voltages, $U_0 = 25$, 30, 35 and 39 kV. For each case, Q increases as t increases until a saturation is reached. The value of the saturation charge Q_s increases with the incident beam energy. With a large incident beam energy, the penetration depth of the incident electron will be larger. We therefore expect the distribution volume of the space charge in the specimen to increase with the beam energy. The arising internal field also depends on the charge distribution and the quantity of trapped charge. Further details on this point will be given in section 6.

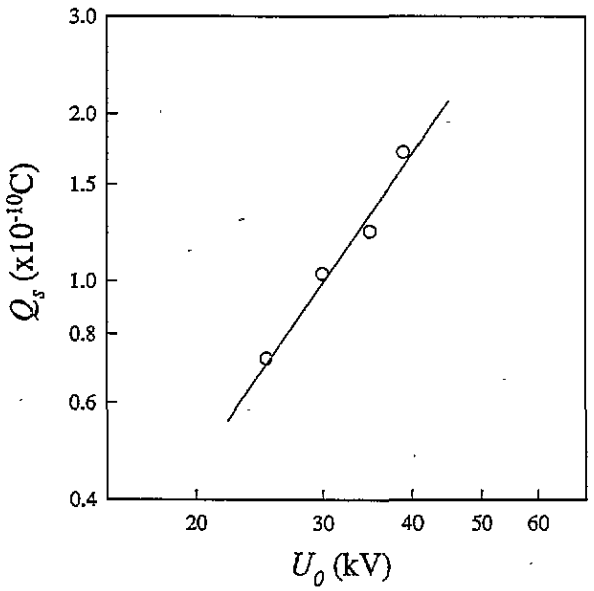

Figure 3. The relation between the saturation charge Q_s and accelerating voltage U_0.

We have also investigated the relationship between Q_s and U_0 and found that a power law relationship is followed as shown in figure 3. The empirical relationship is given as

$$Q_s = kU_0^{1.8} \tag{1}$$

where k is a constant.

5. The internal electric field and discharge process

In the description of the charging stages in section 3, we assert that the self-established internal electric field dominates the charging and discharging processes. Here we verify this point on the basis of experimental observation. During the charging process in the experiment, signals received by the SE detector of the SEM have been recorded. It is found that there are two abrupt increases of the detected signal during the charging process. For example, in the case of charging conditions $I = 1.0 \times 10^{-11}$ A and $U_0 = 39$ keV, two SE signal peaks are observed, one at $t = 10$ s, in the middle of the charging process, and another at $t = 26$ s, just after the saturation. The second peak is higher than the first one.

The increase of the number of electrons collected by the SE detector can be presumably attributed to (i) the increase of the backscattered electrons; (ii) the increase of SE yields due to the decrease of the impact energy of the incident beam electrons decelerated by the surface potential; (iii) the reflection of the incident electrons by the surface potential that is possible as stated in ssection 1; and (iv) the arrival of the detrapped electrons when the internal field established has reached the value of E_c and larger.

We elaborate these possibilities as follows. (i) The backscattered electron coefficient does not change with the impact energy [26, 27] and only a very small number of such electrons reach the SE detector, so this does not contribute to the peaks observed. (ii) Because the increase of the SE yields due to the decrease of impact energy of the incident electrons should change continuously rather than abruptly [26, 27], we can also rule out the second possibility mentioned above. (iii) With the third possibility, if the surface potential due to the early-trapped electrons becomes high enough to reflect the latecoming electrons, there should be one peak in the SE signal rather than two. (iv) The only possibility remaining is the arrival of the detrapped and discharged electrons from the space charge trapped in the specimen. When the internal electric field reaches E_c, charge detrapping happens, which leads to the first peak of the SE signal. As the charging process continues, the internal field increases until it reaches E_m, when the trapped space charge collapses and surface discharge takes place. More electrons are released, so the second peak of the SE signal is higher than the first one. This explanation is in agreement with the fact that surface discharge is observed just after the saturation of the trapped charge is reached.

Therefore we conclude that the internal electric field can reach E_c and E_m earlier than when its corresponding surface potential reaches the value at which the incoming electrons are reflected. The internal electric field is the most important parameter in describing the charging and discharging process. It limits the amount of charge that can be trapped in the specimen and initiates the surface discharge.

6. Calculation of the internal field E_m for surface discharge

We have demonstrated that the self-established field initiates the collapse of the accumulated space charge and induces the surface discharge. In this section, we evaluate this internal field in PMMA through a theoretical hypothesis and the experimental results obtained. From a standard textbook in electrostatics, we learn that the electric field has a maximum value at the edge of the charge distribution if the distribution is in the shape of a disc or a spheroid. However, both disc and spheroid shaped distributions have very sharp edges and are far from realistic. From the result of the Monte Carlo simulation [4, 28], when a fine beam of kiloelectronvolt electrons bombards the specimen, the trapped electrons form a spherical distribution with the region near the beam impact point having a high charge density. With this consideration, we assume a Gaussian distribution, a simple model that may describe the space charge distribution adequately:

$$\rho_e(r) = [Q/(2\pi)^{3/2}\sigma^3]e^{-r^2/2\sigma^2} \tag{2}$$

where Q is the total charge trapped in the specimen and σ the standard deviation. The internal field arising from the charge distribution is then expressed as

$$E(r) = \frac{Q}{(2\pi)^{3/2}\varepsilon_r\varepsilon_0}\frac{1}{\sigma^3 r^2}\int_0^r r^2 e^{-r^2/2\sigma^2}\,dr \tag{3}$$

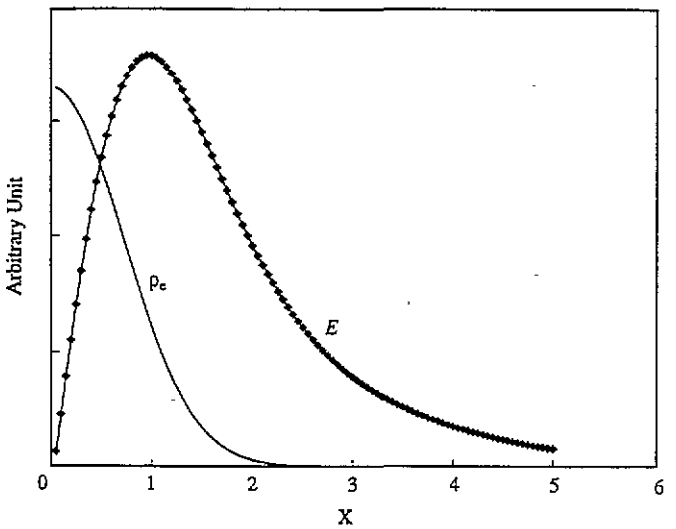

Figure 4. The Gaussian distribution of charge density (ρ_e) and its associated electric field (E).

where $\varepsilon_0 = 8.85 \times 10^{-12}$ C^2 N^{-1} m^{-2}; $\varepsilon_r = 2.6$ is the permittivity of PMMA. By transforming the variable $x \equiv r/\sqrt{2}\sigma$, (3) becomes

$$E(x) = [(Q/4\pi^{3/2}\varepsilon_r\varepsilon_0\sigma^2)/x][[(\sqrt{\pi}/2)/x]\,\mathrm{erf}(x) - \mathrm{e}^{-x^2}] \tag{4}$$

where erf(x) is the error function.

The radial distribution of the electric field, together with the charge distribution, is plotted in figure 4. The position for the maximum field to occur, x_0, is found numerically to be at $x_0 = 0.97$ or $r_0 = 1.37\sigma$. The magnitude of the maximum field is

$$E_{max} = 0.379Q/4\pi^{3/2}\varepsilon_r\varepsilon_0\sigma^2. \tag{5}$$

In the charging process, when Q reaches Q_s, E_{max} reaches E_m, the field initiatiing the surface discharge. However, E_m can be evaluated only when σ is known. In the Gaussian distribution, the standard deviation σ is the measure of the distribution range. Therefore, in our situation of the charge distribution, σ has the meaning of the electron range.

Many experimental methods have been used to measure the charge distribution in insulators [17, 24, 29]. The empirical expressions of the electron penetration range, however, are only obtained by Monte Carlo simulation [26]. Among them the Kanaya–Okayama range [30] is normally used to describe the depth dimension for the interaction volume, and experimental results by Sessler's group [31] show a good agreement with it in the beam energy dependence of the range. The Kanaya–Okayama range (R_{KO}) in units of micrometres is expressed as

$$R_{KO} = 0.0276AU_0^{1.67}/Z^{0.89}d \tag{6}$$

where U_0 is the incident beam energy in kiloelectronvolts, A is the atomic weight in grams per mole, Z is the atomic number, and d is the density in grams per cubic centimetre. For PMMA specimens, the mean atomic number $\bar{Z} = 3.6$, the mean atomic weight $\bar{A} = 6.67$ g mol^{-1}, and the density is measured to be $d = 1.2$ g cm^{-3}. By substituting

Table 1. The saturation charge (Q_s), electron penetration range (R_{KO}), and calculated internal field for surface discharge (E_m) at different beam energies U_0.

	25 kV	30 kV	35 kV	39 kV
Q_s ($\times 10^{-11}$ C)	0.72	1.03	1.23	1.71
R_{KO} (μm)	10.6	14.4	18.6	22.3
E_m (MV cm^{-1})	4.8	3.7	2.6	2.5

σ with R_{KO} and employing the experimental result Q_s for Q in (5), the magnitude of E_m can be calculated. The values of E_m, saturation charge Q_s, and electron range R_{KO} under different charging voltages U_0 are tabulated in table 1. E_m ranges from 2.5 to 4.8 MV cm^{-1}.

The strength of the field E_m initiating the surface discharge in PMMA is higher than the value of 1 MV cm^{-1} that is needed to generate hot electrons to produce an electron cascade. Therefore, it is confirmed once again that, in our charging experiments, the internal electric field can generate electron cascades, initiate the space charge destabilization, and hence induce the surface discharge. One should note that the surface discharge is caused by electrons detrapped by the self-established electric field from a static trapped charge, and the maximum value of E_m is only located in a small region near the edge of the charge area and the field decreases sharply at the neighbourhood (see figure 4), while in the flashover study, surface breakdown is caused by external electric field. Electrons emitted from the triple-junction region (the insulator, cathode, and vacuum) [3] can be accelerated to a high speed before they impinge the insulator surface. So flashover can be produced even when the applied field is much lower. For PMMA, it is in the range of 0.05–0.25 MV cm^{-1} [3].

It is noteworthy that the value of the intrinsic bulk breakdown field is 10 MV cm^{-1} [32] and this value should be the upper limit of the electric field applied to insulators. On the other hand, Zahn's measurement on PMMA samples reports that the bulk breakdown field ranges from 1 to 3.5 MV cm^{-1}. This is because their PMMA samples that are irradiated by high-energy (megaelectronvolt) electron beams. The radiation defects have a significant effect on the breakdown behaviour [33]. The E_m value for surface discharge estimated in the present paper is in the same range as the values reported by Zahn *et al*, but lower than the bulk breakdown field, 10 MV cm^{-1}.

7. Summary

When an insulator is irradiated under a fine kiloelectronvolt electron beam, electrons are trapped in the specimen and a space charge distribution is formed. For a given material, the quantity of the trapped charge approaches the saturation value Q_s as the irradiation time increases. After that, the space charge destabilizes and surface discharge occurs. Q_s depends on the incident beam energy U_0, but not the beam current. Two values of the internal field, namely E_c and E_m, are important in describing the charging and discharging process. At E_c, electrons trapped at the shallow traps or at the edge of the space charge distributions are released. However the detrapping events are relatively small and localized. At E_m, the trapped charge reaches the saturation value, and a relatively large number of trapped electrons is released. The high value of E_m can generate electron cascades and hence destabilize the trapped space charge. The E_m value is estimated by a Gaussian distribution model and it ranges from 2.5 to 4.8 MV cm^{-1} for PMMA specimens.

References

[1] Le Gressus C, Valin F, Henriot M, Gautier M, Duraud J P, Sudarsan T S, Bommakanti R G and Blaise G 1991 *J. Appl. Phys.* **69** 6235

[2] Blaise G and Le Gressus C 1991 *J. Appl. Phys.* **69** 6334

[3] Miller H C 1989 *IEEE Trans. Electr. Insul.* **EI-24** 765

[4] Kotera M and Suga H 1988 *J. Appl. Phys.* **63** 261

[5] Oh K H, Le Gressus C, Gong H, Ong C K, Tan B T G and Ding X Z 1993 *J. Appl. Phys.* **74** 1250

[6] Cazaux J 1986 *J. Appl. Phys.* **59** 1418

[7] Frohlich H, Paranjape B V, Kuper C G and Nakajuna S 1956 *Proc. Phys. Soc.* B **69** 842

[8] O'Dwyer J J 1973 *The Theory of Electrical Conduction and Breakdown in Solid Dielectrics* (Oxford: Clarendon) p 235

[9] Blaise G 1993 *IEEE Trans. Electr. Insul.* **EI-28** 437

[10] Powell C J 1976 *Rev. Mod. Phys.* 46 33

[11] Cartier E, Arnold D and McFeely F R 1992 *Couches Minces* **260** 234

[12] Arnold D, Cartier E and Dimaria D J 1991 *Phys. Rev.* B **45** 1477

[13] Anderson R A 1990 *Proc. XIVth Int. Symp. on Discharge and Electrical Insulation in Vacuum (Santa Fe, NM)* p 311

[14] Dimaria D J, Cartier E and Arnold D 1993 *Proc. Symp. on Amorphous Insulating Thin Films (Boston, MA, 1992)* ed J Kanicki (Pittsburgh, PA: Materials Research Society) p 219

[15] Tanaka R, Sunaga H and Tamura N 1987 *IEEE Trans. Nucl. Sci.* **NS-26** 4670

[16] Zahn M, Hikita M, Wright K A, Cooke C M and Brennan J 1987 *IEEE Trans. Electr. Insul.* **EI-22** 181

[17] Hikita M, Zahn M, Wright K A, Cooke C M and Brennan J 1988 *IEEE Trans. Electr. Insul.* **EI-23** 861

[18] Gong H, Le Gressus C, Oh K H, Ding X Z, Ong C K and Tan B T G 1993 *J. Appl. Phys.* **74** 1944

[19] Chen H, Gong H and Ong C K 1994 *J. Appl. Phys.* 76 806

[20] Le Gressus C and Blaise G 1992 *IEEE Trans. Electr. Insul.* **EI-27** 472

[21] Wetzer J M and Wouters P A A F 1993 *IEEE Trans. Electr. Insul.* **EI-28** 681

[22] Gong H and Ong C K 1994 *J. Appl. Phys.* **75** 449

[23] Vigouroux J P, Duraud J P, Le Moel A, Le Gressus C and Griscom D L 1985 *J. Appl. Phys.* 57 5139

[24] Sessler G M (ed) 1987 *Electrets* 2nd edn (Berlin: Springer) ch 2

[25] Mott N F and Davis E A 1979 *Electronic Processes in Non-Crystalline Materials* 2nd edn (Oxford: Clarendon)

[26] Goldstein J I, Newbury D E, Echlin P, Joy D C, Romig A D Jr, Lyman C E, Fiori C and Lifshin E 1992 *Scanning Electron Microscopy and X-ray Microanalysis* 2nd edn (New York: Plenum) ch 3

[27] Lee R E 1993 *Advanced Scanning Electron Microscopy and X-ray Microanalysis* (New York: Plenum) ch 6

[28] Vicario E, Rosenberg N and Renoud R 1993 *IEEE 1993 Annual Report; Conf. on Electrical Insulation and Dielectric Phenomena* (Windsor: IEEE) p 209

[29] De Reggi A S, Dickens B, Ditchi T, Alquie C, Lewiner J and Lloyd I K 1992 *J. Appl. Phys.* **71** 854

[30] Kanaya K and Okayama S 1972 *J. Phys. D: Appl. Phys.* **5** 43

[31] Lu Tingi and Sessler G M 1991 *IEEE Trans. Electr. Insul.* **EI-26** 228

[32] Cartier E and Pfluger P 1988 *Phys. Scr.* T **23** 235

[33] Clinard F W and Hobbs L W 1986 *Physics of Radiation Effects in Crystals* ed R A Johnson and A N Orlov (Amsterdam: North-Holland) p 444